Article

Kinetics of Photoinduced Electron Transfer between DNA Bases and Triplet 3,3′,4,4′-Benzophenone Tetracarboxylic Acid in Aqueous Solution of Different pH's: Proton-Coupled Electron Transfer?

Truong X. Nguyen,*,†,¶ Daniel Kattnig,† Asim Mansha,† Günter Grampp,*,† Alexandra V. Yurkovskaya,‡ and Nikita Lukzen‡

†Institute of Physical and Theoretical Chemistry, Graz University of Technology, Stremayrgasse 9, 8010 Graz, Austria
‡International Tomography Center, Institutskaya 3a, 630090 Novosibirsk, Russia

Ⓢ Supporting Information

ABSTRACT: The kinetics of triplet state quenching of 3,3′, 4,4′-benzophenone tetracarboxylic acid (BPTC) by DNA bases adenine, adenosine, thymine, and thymidine has been investigated in aqueous solution using time-resolved laser flash photolysis. The observation of the BPTC ketyl radical anion at λ_{max} = 630 nm indicates that one electron transfer is involved in the quenching reactions. The pH-dependence of the quenching rate constants is measured in detail. As a result, the chemical reactivity of the reactants is assigned. The bimolecular rate constants of the quenching reactions between triplet BPTC and adenine, adenosine, thymine, and thymidine are $k_q = 2.3 \times 10^9$ (4.7 < pH < 9.9), $k_q = 4.0 \times 10^9$ (3.5 < pH < 4.7), $k_q = 1.0 \times 10^9$ (4.7 < pH < 9.9), and $k_q = 4.0 \times 10^8$ M^{-1} s^{-1} (4.7 < pH < 9.8), respectively. Moreover, it reveals that in strong basic medium (pH = 12.0) a keto−enol tautomerism of thymine inhibits its reaction with triplet BPTC. Such a behavior is not possible for thymidine because of its deoxyribose group. In addition, the pH-dependence of the apparent electrochemical standard potential of thymine in aqueous solution was investigated by cyclic voltammetry. The $\Delta E/\Delta$pH ≈ −59 mV/pH result is characteristic of proton-coupled electron transfer. This behavior, together with the kinetic analysis, leads to the conclusion that the quenching reactions between triplet BPTC and thymine involve one proton-coupled electron transfer.
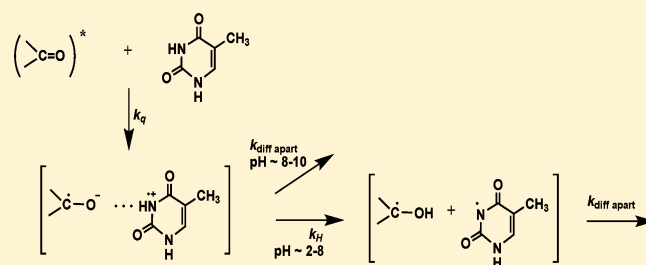
INTRODUCTION

DNA, with its building block DNA bases that store the genetic information, is indispensable in protein biosynthesis. Investigations on long-distance charge transfer through DNA are of ongoing interest.[1−4] Moreover, the interaction of excited triplet states of aromatic carbonyl compounds with DNA bases is also of interest for biophysical and biochemical studies.[3,5,6] These studies may serve as a useful strategy for understanding structure and function of the bases in DNA. In the present study, we want to extend the investigations on the interactions between an aromatic ketone derivative, 3,3′,4,4′-benzophenone tetracarboxylic acid, with selected DNA bases.

3,3′,4,4′-Benzophenone tetracarboxylic acid along with 4-benzophenone monocarboxylic acid (4-BC) are derivatives of benzophenone, and their structures are similar. To get an idea about the kinetics of triplet BPTC, the previous work on 4-BC[7−11] should be considered; however, studies on the photochemical reaction of 4-BC are challenging because of an existing overlap in the spectra of triplet, ketyl radical, and ketyl radical anion between 380 and 720 nm. Although the overlapped spectra of these radicals with similar molar extinction coefficients are comparable, the formation of these radicals also depends on the type of quenchers and radical quantum yields. Therefore, the various absorptions of the radicals need to be considered carefully

when measuring reaction rate constants. In our experiments, we have employed different approaches to analyze these kinetic behaviors.

In this paper, we present the kinetics of the photoreaction of triplet BPTC with various DNA bases in aqueous solution. The pH-dependence of the quenching reaction rate constants is investigated thoroughly for all quenchers. In addition, from cyclic voltammetric measurements, we propose a proton-coupled electron transfer (PCET) by means of a stepwise mechanism from thymine to triplet BPTC.

RESULTS AND DISCUSSION

Before discussing the results, it is helpful to describe first all relevant calculations. As mentioned earlier, two kinetic problems arise when analyzing the data obtained from time-resolved laser flash photolysis: (i) the overlap in the decay of the excited triplet states and the pseudo-first-order growth of the corresponding radicals[12] and (ii) the overlap in the decay of the excited triplet states and the pseudo-first-order growth of the corresponding radicals and their simultaneous

second-order decay.[13] To deal with these kinetics, we applied two alternative approaches.
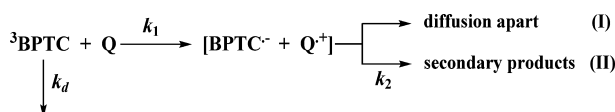
According to the low concentrations of BPTC (1×10^{-4} mol L^{-1}) used, triplet–triplet annihilation is negligible. The interaction of triplet BPTC with quencher is a pseudo-first-order reaction. Thereupon, the observed quenching rate constant, k_q^{obs}, is obtained by monitoring the triplet decay of BPTC at fixed wavelengths, applying the Stern–Volmer relation, eq 1a or eq 1b:

$$k_{obs} = k_d + k_q^{obs}[Q] \quad (1a)$$

$$\frac{^3\tau_0}{^3\tau} = 1 + {}^3\tau_0 k_q^{obs}[Q] \quad (1b)$$

Here, k_d is the decay rate constant of triplet BPTC; k_q^{obs} is the observed quenching rate constant. $^3\tau_0 = (1/k_d)$ is the lifetime of triplet BPTC in the absence of quencher; $^3\tau = (1/k_{obs})$ is actual lifetime of triplet BPTC in the presence of quencher. $[Q]$ stands

Scheme 1. Two kinetic problems considered

$$^3\text{BPTC} + \text{Q} \xrightarrow{k_1} [\text{BPTC}^{\cdot-} + \text{Q}^{\cdot+}] \longrightarrow \begin{array}{l} \text{diffusion apart} \quad (I) \\ \xrightarrow{k_2} \text{secondary products} \quad (II) \end{array}$$

$$\Big\downarrow k_d$$

for the quencher concentration. Reaction Scheme 1 illustrates the two kinetic problems, where k_1 is the first-order growth of radicals,

$$k_1 = k_q^{obs}[Q] \quad (2)$$

and k_2 is the second-order rate of the disappearance of radicals:

(i) If the system shows a combination of parallel reactions, a decay process and the first-order growth of radicals (pathway I, Scheme 1, denoted here as model I), the following equation applies:

$$\ln \frac{A - A^\infty}{A^0 - A^\infty} = -k_{obs}t \quad (3)$$

where A^0, A, and A^∞ are the absorbances at time 0, t, and infinity, respectively. Using k_{obs} obtained from eq 3 and employing eq 1b with various concentrations of the quencher gives values of k_q^{obs}.

(ii) If the system shows a combined decay process, a first-order growth of radicals and an overlap by their simultaneous second-order decay (pathway II, Scheme 1, denoted here as model II), the time-resolved absorbance for the system is expressed by eq 4

$$\frac{dA}{dt} = \frac{dA^{^3\text{BPTC}}}{dt} + \frac{dA^{\text{BPTC}^{\bullet-}}}{dt} \quad (4)$$

and

$$\frac{d[^3\text{BPTC}]}{dt} = -(k_d + k_1)[^3\text{BPTC}] \quad (5)$$

$$\frac{d[\text{BPTC}^{\bullet-}]}{dt} = k_1[^3\text{BPTC}] - k_2[\text{BPTC}^{\bullet-}]^2 \quad (6)$$

Thus, taking k_1 obtained from the simulation, eqs 4–6, and applying eq 2 with various concentrations of the quencher gives the value of k_q^{obs}.

pH-Dependence of the Observed Quenching Rate Constant. The observed quenching rate constant is expressed according to the suggestion of Yurkovskaya et al.,[14] with the assumption that a polyprotic acid symbolized by H$_n$A, initial concentration C_0 can undergo n-proton dissociation in water and form the corresponding base conjugates. Each step has its own

dissociation constant, K_{aj}, $j = 1, .., n$. The fraction of each species is given by eq 7,

$$[\text{H}_{n-k}\text{A}]/C_0 = \Big([\text{H}^+]^{n-k}\prod_{j=0}^{k} K_{aj}\Big)\Big/\Big(\sum_{k=0}^{n}[\text{H}^+]^{n-k}\prod_{j=0}^{k} K_{aj}\Big) \quad (7)$$

with $0 \leq j \leq k$; $0 \leq k \leq n$; $K_{a0} = 1$.

For example, for triplet BPTC, $pK_{a1}^* = 2.1$ and $pK_{a2}^* = 4.7$ (see the text), whereas for thymine, $pK_a = 9.9$.[15] The molar fractions, depicted in Figure 1, of all species in the solution are, hence,

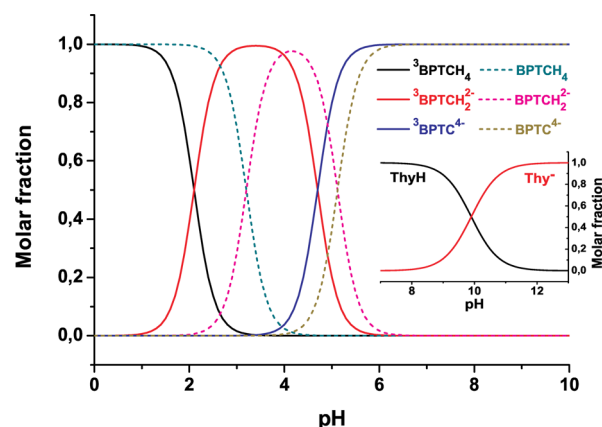**Figure 1.** Molar fractions of BPTC, ^{3}BPTC, and thymine in the solution.

calculated by eq 7. The pH-dependence of k_q^{obs} for the reaction of triplet BPTC with thymine is then divided into four regions on the basis of their pK_a values and molar fractions:[14]

pH < 2.1 ^{3}BPTCH$_4$ and ThyH k_{q1}

2.1 < pH < 4.7 ^{3}BPTCH$_2^{2-}$ and ThyH k_{q2}

4.7 < pH < 9.9 ^{3}BPTC^{4-} and ThyH k_{q3}

9.9 < pH ^{3}BPTC^{4-} and Thy$^-$ k_{q4}

Each pair of reactants is characterized by the so-called intrinsic quenching rate constant k_{qi} ($i = 1 ... 4$), and the k_q^{obs} can be treated as a summation of k_{qi} multiplied by the molar fraction of the corresponding species according to eq 8. Further details of this equation can be found in the Supporting Information.

$$\begin{aligned} k_q^{obs} &= k_{q1}\frac{[\text{H}^+]^4}{[\text{H}^+]^4 + [\text{H}^+]^2 K_{a1}^{*2} + K_{a1}^{*2}K_{a2}^{*2}} \times \frac{[\text{H}^+]}{[\text{H}^+] + K_a} \\ &+ k_{q2}\frac{[\text{H}^+]^2 K_{a1}^{*2}}{[\text{H}^+]^4 + [\text{H}^+]^2 K_{a1}^{*2} + K_{a1}^{*2}K_{a2}^{*2}} \times \frac{[\text{H}^+]}{[\text{H}^+] + K_a} \\ &+ k_{q3}\frac{K_{a1}^{*2}K_{a2}^{*2}}{[\text{H}^+]^4 + [\text{H}^+]^2 K_{a1}^{*2} + K_{a1}^{*2}K_{a2}^{*2}} \times \frac{[\text{H}^+]}{[\text{H}^+] + K_a} \\ &+ k_{q4}\frac{K_{a1}^{*2}K_{a2}^{*2}}{[\text{H}^+]^4 + [\text{H}^+]^2 K_{a1}^{*2} + K_{a1}^{*2}K_{a2}^{*2}} \times \frac{K_a}{[\text{H}^+] + K_a} \end{aligned} \quad (8)$$

Finally, a multiple regression employed on eq 8 with known parameters (k_q^{obs}, K_{aj}, K_{aj}^*, $[\text{H}^+]$) estimates the intrinsic values, k_{qi}.

Similar expressions of the pH-dependence of the observed quenching rate constants were applied for photochemical reactions of BPTC with the other quenchers.

Absorption Spectra. Absorption spectra of BPTC recorded in the absence and in the presence of thymine are shown in Figure 2. It is likely that there is no association between BPTC
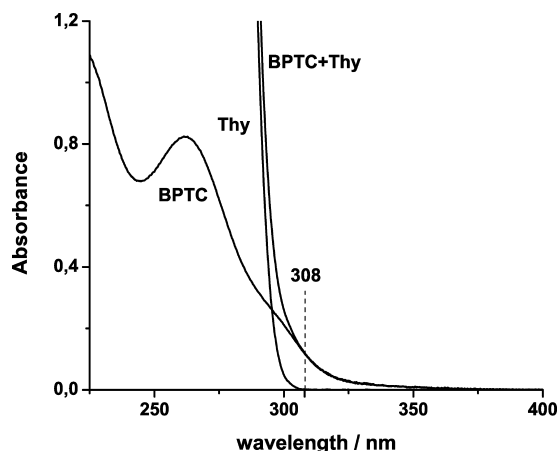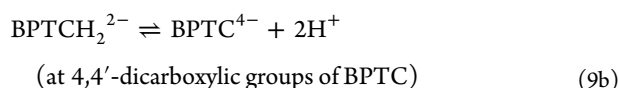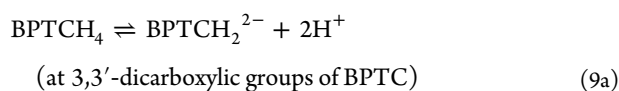

Figure 2. Absorption spectra of BPTC (4×10^{-5} mol L^{-1}) without and with thymine (1.5×10^{-3} mol L^{-1}) in water at pH = 2.0.

and thymine in the ground state, since the spectrum of the mixture of both shows an addition of their separate spectra. Similar behaviors are observed with the other quenchers at different pH's.

By changing the pH of the solution, it is possible to control which main reactant species are present in the solution. Therefore, it is important to know the pK_a values. Using UV−vis spectroscopic measurements, we determined that BPTC has two pK_a values: pK_{a1} = 3.20 ± 0.10 and pK_{a2} = 5.12 ± 0.10.[16] The fact that only two pK_a values are observed implies that there are two deprotonation steps of BPTC characterized by two-proton dissociation for each. We suggest the following acid−base equilibria:

$$BPTCH_4 \rightleftharpoons BPTCH_2{}^{2-} + 2H^+$$

(at 3,3′-dicarboxylic groups of BPTC)   (9a)

$$BPTCH_2{}^{2-} \rightleftharpoons BPTC^{4-} + 2H^+$$

(at 4,4′-dicarboxylic groups of BPTC)   (9b)

On the basis of the pK_a values and contribution of species (Figure 1, dashed lines), it is unambiguous that eq 9a predominates at pH > 3.2, whereas eq 9b dominates at pH > 5.1. BPTCH$_2{}^{2-}$ is the main species present at pH ∼ 4.1.

Deprotonated forms of BPTC show absorption spectra at longer wavelengths compared with its neutral state. BPTCH$_4$ is found to have an absorption maximum at 261 nm (at pH = 2.1), whereas the spectrum of BPTCH$_2{}^{2-}$ is shifted to 269.5 nm (pH = 4.1). BPTC^{4-} shows a maximum at 276.5 nm (pH = 12.0).

Transient Absorption Spectra. Laser flash photolysis of BPTC (1×10^{-4} mol L^{-1}) in aqueous solutions at pH = 2.0 and 12.0 gives spectra as Figure 3. They are very similar to the triplet spectra reported for benzophenone and 4-BC.[7] Triplet BPTC shows a strong absorption peak at λ_{max} = 590 nm in water at pH = 2.0, shifting to λ_{max} = 550 nm at pH = 12.0. Because of these results, we have chosen 590 and 550 nm as observation wavelengths for kinetic traces of all quenching experiments in the
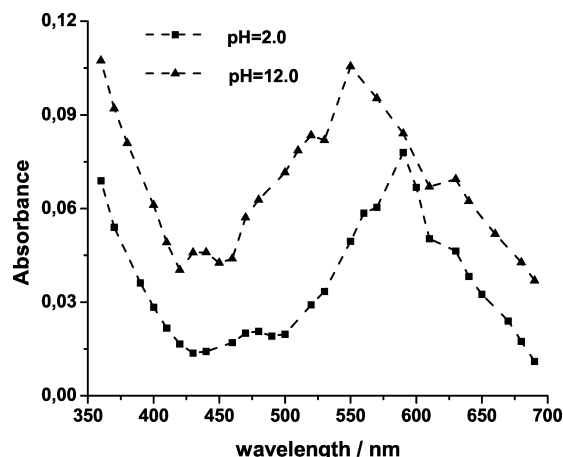

Figure 3. Transient absorption spectra of BPTC (1×10^{-4} mol L^{-1}) in water, monitored by transient absorbances between 360 and 690 nm obtained right after laser flash.

acidic media and in the basic media, respectively. The decay of triplet BPTC, observed at both wavelengths λ_{max} = 590 and 550 nm in water follows a first-order kinetics with k_d = (5−7) × 10^5 s^{-1}, in agreement with reported values[17,18] (7.1 × 10^5 and 6.8 × 10^5 s^{-1}).

Determination of pK_a^*. Because two pK_a values are observed in the ground state, it is expected that BPTC also behaves in the same way in the excited triplet state. We estimated the pK_a^* of triplet BPTC by triplet−triplet absorbance titration.[19] The pH-dependence of the absorbance ratio at 590 and 550 nm obtained immediately after laser flash is shown in Figure 4. The pK_a^* values
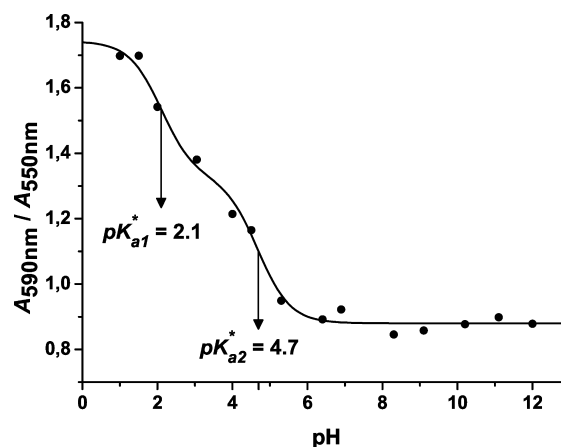
Figure 4. Triplet−triplet absorbance titration curve of 1×10^{-4} mol L^{-1} BPTC in water, monitored by the ratio of transient absorbances at 590 and 550 nm, obtained right after laser flash. Solid line: calculation with the pK_a^* values 2.1 and 4.7.

for triplet BPTC are determined from the turning points of this $T_1 \rightarrow T_n$ absorbance titration curve as pK_{a1}^* = 2.1 ± 0.2 and pK_{a2}^* = 4.7 ± 0.2. This indicates that triplet BPTC is a stronger acid in comparison with its ground-state one.

It is realized in Figure 1 that ^{3}BPTCH$_4$ exits mainly in the solution of pH < 2.1, whereas its dianionic ^{3}BPTCH$_2{}^{2-}$ dominates within 2.1 < pH < 4.7. Note here that at pH = 3.2, for instance, the light-absorbing species could be both neutral BPTCH$_4$ and dianionic BPTCH$_2{}^{2-}$, which then generate their corresponding triplet states. However, 308 nm irradiation of BPTC solutions at

pH = 3.2 results in the main species $^3\text{BPTCH}_2^{2-}$ because of the rapid acid−base equilibrium eq 10.

$$^3\text{BPTCH}_4 \rightleftharpoons {}^3\text{BPTCH}_2^{2-} + 2\text{H}^+ \tag{10}$$
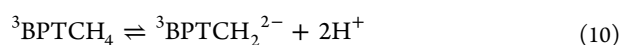
Otherwise, at pH > 4.7 the species $^3\text{BPTC}^{4-}$ is mainly present because of the rapid equilibrium eq 11 although BPTCH_2^{2-} could be initially excited (e.g., at pH = 5.1).

$$^3\text{BPTCH}_2^{2-} \rightleftharpoons {}^3\text{BPTC}^{4-} + 2\text{H}^+ \tag{11}$$
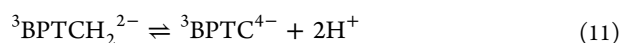
Quenching Experiments of Triplet BPTC. As already pointed out, all experimental traces for triplet BPTC decay were monitored at $\lambda_{\text{obs}} = 590$ nm in acid solutions and at $\lambda_{\text{obs}} = 550$ nm in alkaline solutions, respectively. All experimental data for the measured quenching rate constants were fitted with either model I or model II.

Quenching by Thymine. Triplet BPTC and thymine can exist in either neutral or deprotonated forms, depending on the pH of the solution (see Table 1). In the presence of thymine, the

Figure 5. Decays ($\lambda_{\text{obs}} = 590$ nm) of triplet BPTC (1×10^{-4} mol L^{-1}) + Thy (concentration increases from top to bott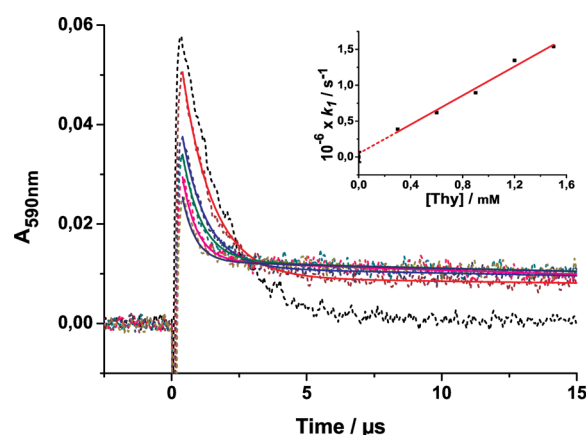om: 0−1.5 mM) in water at pH = 6.4. Experimental, dashed lines; simulation with eq 4, solid lines. Inset: k_1 vs [Thy] plot.

Table 1. Quenching Rate Constants of BPTC Triplet by Quenchers (k_{qi})

quencher	pH region	reactant pair	k_{qi}	k_{qi} (mol^{-1}L s^{-1})
adenine	pH < 2.1	$^3\text{BPTCH}_4$ and AdeH_2^+	k_{q1}	0
	2.1 < pH < 4.2	$^3\text{BPTCH}_2^{2-}$ and AdeH_2^+	k_{q2}	8.4×10^9
	4.2 < pH < 4.7	$^3\text{BPTCH}_2^{2-}$ and AdeH	k_{q3}	2.0×10^9
	4.7 < pH < 9.9	$^3\text{BPTC}^{4-}$ and AdeH	k_{q4}	2.3×10^9
	9.9 < pH	$^3\text{BPTC}^{4-}$ and Ade$^-$	k_{q5}	4.7×10^8
adenosine	pH < 2.1	$^3\text{BPTCH}_4$ and dAdeH_2^+	k_{q1}	4.8×10^9
	2.1 < pH < 3.5	$^3\text{BPTCH}_2^{2-}$ and dAdeH_2^+	k_{q2}	6.8×10^9
	3.5 < pH < 4.7	$^3\text{BPTCH}_2^{2-}$ and dAdeH	k_{q3}	4.0×10^9
	4.7 < pH < 12.5	$^3\text{BPTC}^{4-}$ and dAdeH	k_{q4}	6.2×10^8
	12.5 < pH	$^3\text{BPTC}^{4-}$ and dAde$^-$	k_{q5}	4.5×10^7
thymine	pH < 2.1	$^3\text{BPTCH}_4$ and ThyH	k_{q1}	3.5×10^9
	2.1 < pH < 4.7	$^3\text{BPTCH}_2^{2-}$ and ThyH	k_{q2}	2.5×10^9
	4.7 < pH < 9.9	$^3\text{BPTC}^{4-}$ and ThyH	k_{q3}	1.0×10^9
	9.9 < pH	$^3\text{BPTC}^{4-}$ and Thy$^-$	k_{q4}	0
thymidine	pH < 2.1	$^3\text{BPTCH}_4$ and dThyH_2	k_{q1}	6.6×10^9
	2.1 < pH < 4.7	$^3\text{BPTCH}_2^{2-}$ and dThyH_2	k_{q2}	2.5×10^9
	4.7 < pH < 9.8	$^3\text{BPTC}^{4-}$ and dThyH_2	k_{q3}	4.0×10^8
	9.8 < pH < 12.9	$^3\text{BPTC}^{4-}$ and dThyH$^-$	k_{q4}	3.1×10^8
	12.9 < pH	$^3\text{BPTC}^{4-}$ and dThy^{2-}	k_{q5}	0^a

$^a k_{q5} = 0$ implies that the deprotonation of the deoxyribose group of dThy do not much influence the overall quenching rate constant.

Figure 6. BPTC ketyl radical anion spectrum in the presence of thymine (1.5×10^{-2} mol L^{-1}) at pH = 2.0. Inset: decay profile ($\lambda_{\text{obs}} = 630$ nm) of BPTC$^{\bullet-}$, which forms pinacol after the fast protonation of BPTC$^{\bullet-}$ to BPTCH·.

lifetime of triplet BPTC is decreased, and the long-lived BPTC ketyl radical anion (BPTC$^{\bullet-}$) appears, $\lambda_{\text{max}} = 630$ nm (see below). The formation of the ketyl radical anion implies that the photochemical primary step is an electron transfer. In the range of pH = 2.0−10.0, we found that the transient kinetics for this system correspond to model II. Data analysis for this system by model II in the solution of pH = 6.4 is presented in Figure 5.

It can be seen that the total radical absorbance is high ($A_{\text{radical}}^{\infty}/A_{\text{triplet}}^0 = 0.29$) with [Thy] = 6×10^{-4} mol L^{-1} (Figure 5) as a result of the high radical quantum yield of BPTC$^{\bullet-}$ at pH = 6.4. Plotting k_1 vs [Thy] at pH = 6.4 (Figure 5, inset) gives a good linearity and zero intercept, showing that the model accurately describes the kinetic behavior. The spectrum of BPTC$^{\bullet-}$ over the range of 610−660 nm was obtained by laser flash irradiation of the solution of BPTC (1.0×10^{-4} mol L^{-1}) and thymine ($1.5 \times$

10^{-2} mol L^{-1}) (Figure 6). BPTC$^{\bullet-}$ absorbs at $\lambda_{\text{max}} = 630$ nm, and the decay monitored at $\lambda_{\text{obs}} = 630$ nm obeys a second-order kinetics ($k_2/\varepsilon_{\text{BPTC}^{\bullet-}} = 3 \times 10^5$ cm s^{-1}). In addition, Inbar et al.[7] reported that the pinacol yield of the 4-BC$^{\bullet-}$ + 4-BC$^{\bullet-}$ reaction is minor. These lead to the postulation that after an initial electron transfer followed by proton transfer, ketyl radicals (BPTCH·) are formed, which dissociate into free radical ions and thereafter randomly encounter to undergo the pinacol reaction (BPTCH· + BPTCH·).

On the other hand, the formation of BPTC$^{\bullet-}$ could not be observed at pH = 12.0, even at high concentrations of thymine ([Thy] = 1.5×10^{-2} mol L^{-1}). This can be explained by the keto−enol tautomerism of Thy$^-$ (Scheme 2), which significantly changes the chemical properties of Thy$^-$. In addition, it is possible that the proton transfer from the oxidized thymine is strongly hindered at pH = 12.0 and the electron reverts back to the thymine molecule instead of remaining on the BPTC. Therefore, no quenching reaction of triplet BPTC by Thy$^-$ occurs (i.e., in eq 8, $k_{q4} = 0$).

The pH-dependence of the observed quenching rate constants is presented in Figure 7. Although the quenching reaction follows

Scheme 2. Tautomerism of Thymine at pH > 10

Keto form   Enol form   Rearranged enol form

Figure 7. pH-dependence of the observed quenching rate constant for the reaction of triplet BPTC with thymine. The solid line is the simulation according to eq 8 with $k_{q4} = 0$. See Table 1 for parameters.

Figure 8. pH-dependence of the observed quenching rate constant for the reaction of triplet BPTC with dThy. Solid line is a simulation from eq 12.

a complex reaction system that shows multiple (de)protonation equilibria in the ground and excited states, the pH-dependent k_q^{obs} is adequately established. Figure 7 depicts a continuous downhill and flat behavior of k_q^{obs}. The decrease in k_q^{obs} with pH is characterized by two changes (at pH ≈ 2.1 and 4.7) which coincide with the two-deprotonation stages of triplet BPTC. Moreover, k_q^{obs} reaches plateaus in the regions,

$$3 < \text{pH} < 4 \; (^{3}\text{BPTCH}_2{}^{2-} + \text{ThyH}) \quad \text{and}$$

$$6 < \text{pH} < 8 \; (^{3}\text{BPTC}^{4-} + \text{ThyH})$$

that are attributed to the equilibria of the corresponding reactant pairs. Note that in the range of pH < pK_a, thymine exists in the neutral form (Figure 1, inset) and triplet BPTC shows two steps of deprotonation ($pK_{a1}^* = 2.1$ and $pK_{a2}^* = 4.7$). Therefore, it allows the prediction of the chemical reactivity between triplet BPTC and thymine in the order

$$^{3}\text{BPTCH}_4 > {}^{3}\text{BPTCH}_2{}^{2-} > {}^{3}\text{BPTC}^{4-}$$

Perhaps, for a more negative net charge, the reduction is more difficult and the quenching rate constant becomes lower.

Quenching by Thymidine. Within the pH range of 2.0−12.0, the decay of triplet BPTC in the presence of dThy obeys model I. The appearance of the long-lived transient (BPTC•−) at λ_{obs} = 630 nm is observed, which then decays according to a second-order kinetics on the milliseconds time scale. This is interpreted by an electron transfer mechanism from dThy to triplet BPTC, forming the radical pair followed by fast escape of these radical ions from the charge-transfer successor complex. Thereafter, depending on pH of the solution, the pinacol reactions, BPTCH· + BPTCH·, BPTCH· + BPTC•−, or BPTC•−+BPTC•− occur. Note that unlike thymine, a keto−enol tautomerism is no longer achieved due to the deoxyribose group of thymidine.

The pH-dependence of k_q^{obs} can be expressed by eq 12 and is presented in Figure 8 (see Tables 1 and 2 for parameters).

$$
\begin{aligned}
k_q^{obs} = \; & k_{q1} \frac{[\text{H}^+]^4}{[\text{H}^+]^4 + [\text{H}^+]^2 K_{a1}^{*2} + K_{a1}^{*2} K_{a2}^{*2}} \\
& \times \frac{[\text{H}^+]^2}{[\text{H}^+]^2 + [\text{H}^+]K_{a1} + K_{a1}K_{a2}} \\
& + k_{q2} \frac{[\text{H}^+]^2 K_{a1}^{*2}}{[\text{H}^+]^4 + [\text{H}^+]^2 K_{a1}^{*2} + K_{a1}^{*2} K_{a2}^{*2}} \\
& \times \frac{[\text{H}^+]^2}{[\text{H}^+]^2 + [\text{H}^+]K_{a1} + K_{a1}K_{a2}} \\
& + k_{q3} \frac{K_{a1}^{*2} K_{a2}^{*2}}{[\text{H}^+]^4 + [\text{H}^+]^2 K_{a1}^{*2} + K_{a1}^{*2} K_{a2}^{*2}} \\
& \times \frac{[\text{H}^+]^2}{[\text{H}^+]^2 + [\text{H}^+]K_{a1} + K_{a1}K_{a2}} \\
& + k_{q4} \frac{K_{a1}^{*2} K_{a2}^{*2}}{[\text{H}^+]^4 + [\text{H}^+]^2 K_{a1}^{*2} + K_{a1}^{*2} K_{a2}^{*2}} \\
& \times \frac{[\text{H}^+]K_{a1}}{[\text{H}^+]^2 + [\text{H}^+]K_{a1} + K_{a1}K_{a2}} \\
& + k_{q5} \frac{K_{a1}^{*2} K_{a2}^{*2}}{[\text{H}^+]^4 + [\text{H}^+]^2 K_{a1}^{*2} + K_{a1}^{*2} K_{a2}^{*2}} \\
& \times \frac{K_{a1}K_{a2}}{[\text{H}^+]^2 + [\text{H}^+]K_{a1} + K_{a1}K_{a2}} \quad (12)
\end{aligned}
$$

The main reactions at each pH region and their corresponding quenching rate constants, k_{qi}, obtained by the best fit (solid line, Figure 8), are summarized in Table 1. Note also that $k_{q5} = 0$ implies that the deprotonation of the deoxyribose group ($pK_a = 12.9$) of dThy does not much influence the overall quenching

Table 2. List of Compounds

Compound	Abbreviation	Structure	pK_a
3,3',4,4'-benzophenone-tetracarboxylic acid	BPTC		2.1; 4.7[a]
Thymine	Thy		9.9[b]
Thymidine	dThy		9.8; 12.9[b]
Adenine	Ade		4.2; 9.9[c]
Adenosine	dAde		3.5; 12.5[c]

[a]For the triplet state. [b]Ref 15. [c]Ref 24.

rate constant. Therefore, a similar explanation, such as the quenching reaction by thymine for pH < 10, is given for the variation of k_q^{obs} with pH. A further decrease in k_q^{obs} at pH > 10 is caused by the shift of the dThyH2 equilibrium toward its anionic form. An effect of Coulombic repulsion may hinder the encounter of ^{3}BPTC^{4-} and result in dThyH$^-$; hence, the quenching rate constants get smaller.

Quenching by Adenine. The reactive species existing in solution at different pH's are shown in Table 1. For the whole range of pH = 2.0–12.0, we found that the decay of triplet BPTC in the presence of Ade follows model I with the formation of BPTC$^{\bullet-}$. The appearance of transient BPTC$^{\bullet-}$ leads to the conclusion that an electron transfer reaction from Ade to triplet BPTC is followed by fast diffusion of the reactants.

The pH-dependence of k_q^{obs} is described by eq 13 and is presented in Figure 9 (see Tables 1 and 2 for parameters).

$$
\begin{aligned}
k_q^{obs} = {} & k_{q1}\frac{[H^+]^4}{[H^+]^4 + [H^+]^2 K_{a1}^{*2} + K_{a1}^{*2}K_{a2}^{*2}} \\
& \times \frac{[H^+]^2}{[H^+]^2 + [H^+]K_{a1} + K_{a1}K_{a2}} \\
& + k_{q2}\frac{[H^+]^2 K_{a1}^{*2}}{[H^+]^4 + [H^+]^2 K_{a1}^{*2} + K_{a1}^{*2}K_{a2}^{*2}} \\
& \times \frac{[H^+]^2}{[H^+]^2 + [H^+]K_{a1} + K_{a1}K_{a2}} \\
& + k_{q3}\frac{[H^+]^2 K_{a1}^{*2}}{[H^+]^4 + [H^+]^2 K_{a1}^{*2} + K_{a1}^{*2}K_{a2}^{*2}} \\
& \times \frac{[H^+]K_{a1}}{[H^+]^2 + [H^+]K_{a1} + K_{a1}K_{a2}} \\
& + k_{q4}\frac{K_{a1}^{*2}K_{a2}^{*2}}{[H^+]^4 + [H^+]^2 K_{a1}^{*2} + K_{a1}^{*2}K_{a2}^{*2}} \\
& \times \frac{[H^+]K_{a1}}{[H^+]^2 + [H^+]K_{a1} + K_{a1}K_{a2}} \\
& + k_{q5}\frac{K_{a1}^{*2}K_{a2}^{*2}}{[H^+]^4 + [H^+]^2 K_{a1}^{*2} + K_{a1}^{*2}K_{a2}^{*2}} \\
& \times \frac{K_{a1}K_{a2}}{[H^+]^2 + [H^+]K_{a1} + K_{a1}K_{a2}}
\end{aligned}
\tag{13}
$$

It is seen that $k_{q1} = 0$, which implies no quenching reaction of triplet BPTC by AdeH$_2^+$ under strong acidic conditions (pH < 2). Figure 9
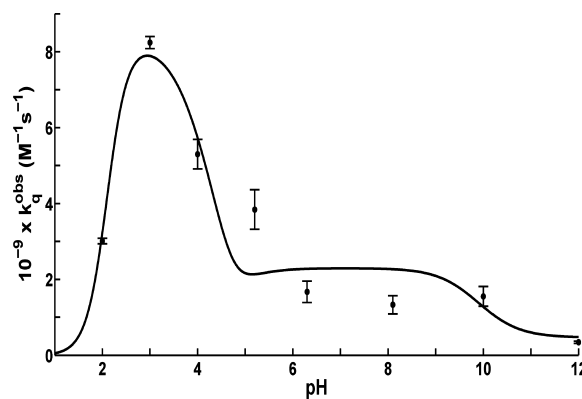

Figure 9. pH-dependence of the observed quenching rate constant for the reaction of triplet BPTC with dAde. The solid line is a simulation from eq 13.

shows a maximum of k_q^{obs} at pH $\approx$ 2.8. The increase in k_q^{obs} up to pH $\approx$ 2.8 can be explained by a shift of the triplet BPTC equilibrium toward its dianionic form,[20] eq 10. The main reactant pair within 2.1 < pH < 4.2 is ^{3}BPTCH$_2^{2-}$ + AdeH$_2^+$. Thus, the maximum quenching rate constant here can be attributed to the molecular net charge of the reactants (Coulombic interaction). The further decrease in k_q^{obs} at pH $\approx$ 2.8−5 is caused by a drop in the AdeH$_2^+$ concentration following the equilibrium as eq 14:

$$\text{AdeH}_2^+ \rightleftharpoons \text{AdeH} + \text{H}^+ \tag{14}$$

At pH > 5, an explanation similar to that of the quenching reaction by thymidine for the change of k_q^{obs} with pH is used.

Quenching by Adenosine. The decay profile and kinetic analysis for the quenching of triplet BPTC by dAde at pH = 4.0 is shown in Figure 10. It can be seen that the total radical
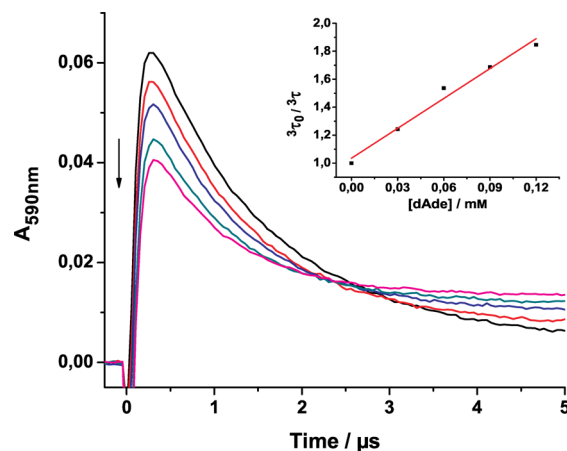

Figure 10. Decay profiles (λ_{obs} = 590 nm) for the BPTC + dAde system in water at pH = 4.0. Concentration of dA increases from top to bottom: 0−0.12 mM. Inset: Stern−Volmer plot from eqs 3 and 1b.

absorbance increases slightly with the concentration of dAde. Kinetic treatment by model I within the range of pH = 2.0−12.0 is applied. Together with the observation of BPTC$^{\bullet-}$ at λ_{obs} = 630 nm, it leads to the conclusion that electron transfer from dAde to triplet BPTC occurs, followed by a fast diffusion step. The pH-dependence of k_q^{obs} is expressed by eq 13 (see Tables 1 and 2 for parameters). Values obtained from the best fit (solid line, Figure 11) are summarized in Table 1. Once again, an explanation similar to
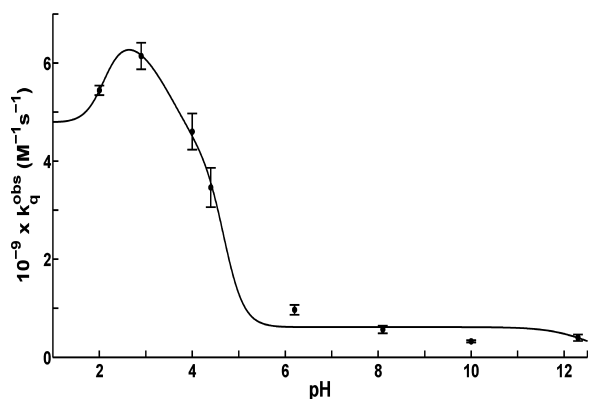
Figure 11. pH-dependence of k_q^{obs} for the reaction of triplet BPTC with dAde. The solid line is a simulation from eq 13.

that of the quenching reaction by adenine for the variation of k_q^{obs} with pH is used.

Cyclic Voltammetric Investigation. One question remains that is related to the quenching reactions of triplet BPTC by thymine at pH = 2.0−10: Is electron transfer followed by proton transfer? To check the possibility, we have investigated the pH-dependence of the oxidation potential of thymine by cyclic voltammetry. Whatever the reaction mechanism may be, a global Nernst equation can be applied for the thermodynamics of the redox reaction:[21]

$$E = E_{ap}^{0,ox/red} + \frac{RT}{nF} \ln \frac{\sum [\mathrm{ox}]}{\sum [\mathrm{red}]} \qquad (15)$$

Here, E is the electrode potential; $E_{ap}^{0,ox/red}$ is the apparent standard oxidation potential of the corresponding redox couple; and $\sum [\mathrm{ox}]$ and $\sum [\mathrm{red}]$ are the total concentrations of the oxidized and reduced species in solution, respectively. Therefore, the pH-dependence of E_{ap}^0 for the oxidation of thymine can be described by eq 16 (see the Supporting Information), as shown in Figure 12.
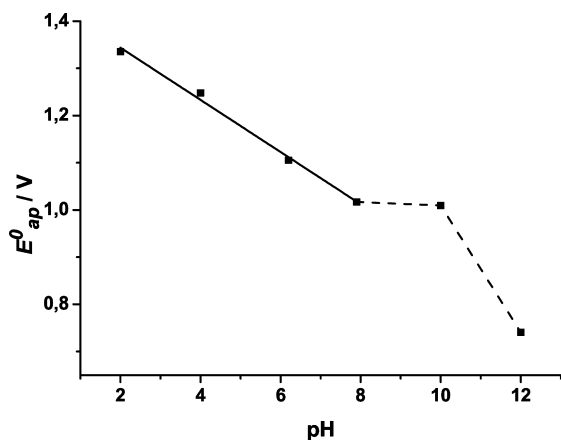

Figure 12. The apparent oxidation potential vs Ag/AgCl of thymine (1 mM) as a function of pH. Solid line: linear fitting with a slope of −55.2 mV/pH.

$$E_{ap}^0 = E_{\mathrm{ThyH}^{\bullet+}/\mathrm{ThyH}}^0 - 0.059(\mathrm{pH} - \mathrm{p}K_{a,\mathrm{ThyH}^{\bullet+}}) \qquad (16)$$

Here, $\mathrm{p}K_{a,\mathrm{ThyH}^{\bullet}} = 3.2$ is the dissociation constant of thymine radical cation.[22]

Between pH = 2−8, E_{ap}^0 shows a linear variation with pH, together with the characteristic slope of approximately −59 mV per pH unit. This indicates a one-proton-coupled one-electron transfer during the oxidation of thymine.[23] This observation and the above kinetic analysis of the quenching reaction by thymine suggest that the possible pathway of the quenching reaction of triplet BPTC by thymine at pH around 2−8 is initially an electron transfer, followed by proton transfer (Scheme 3). At pH around 8−10, a simple electron transfer mechanism might take place in competition.

Scheme 3. Quenching Reaction of Triplet BPTC by Thymine
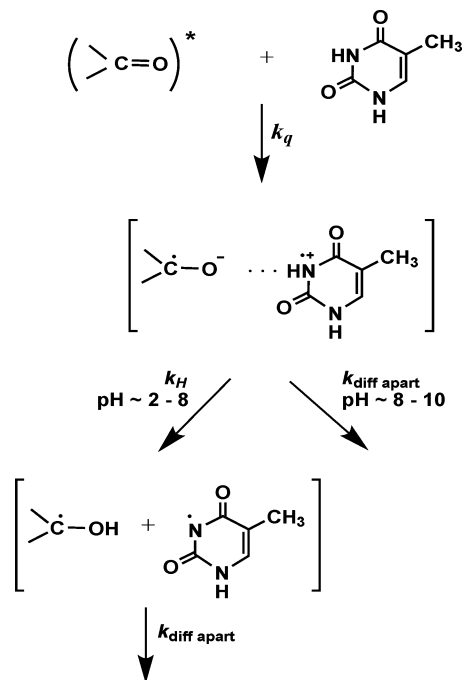
■ CONCLUSION

The quenching of the triplet state of 3,3′,4,4′-benzophenone tetracarboxylic acid by DNA bases in aqueous solution was investigated using time-resolved laser flash photolysis. The observation of the BPTC ketyl radical anion (λ_{max} = 630 nm) confirms that the primary photochemical step is electron transfer. Although the forms of the triplet BPTC and quenchers depend on the pH of the solution, we have been able to establish a relationship of the quenching rate constant of each pair of reactants with the overall quenching rate constant.

Particularly, the pH-dependence of the apparent standard potential of thymine in aqueous solution was investigated by cyclic voltammetry. From the kinetic analysis of the quenching reactions, the pH-dependent oxidation potential of thymine indicates that proton-coupled electron transfer by means of a stepwise mechanism from thymine to triplet BPTC in the solutions of pH ≈ 2−8 proceeds. In the strong basic solution (pH = 12.0), no quenching reaction between triplet BPTC and thymine takes place, whereas it is observed for thymidine. This can be explained by a keto−enol tautomerism, which changes the chemical properties of thymine. Such a tautomerism is not possible for thymidine because of its deoxyribose group.

10674

dx.doi.org/10.1021/jp307122h | J. Phys. Chem. A 2012, 116, 10668−10675

■ EXPERIMENTAL SECTION

Materials. The abbreviations used in this article can be found in the section Results and Discussion. 3,3′,4,4′-Benzophenone tetracarboxylic acid is a generous gift from Dr. Y. Lin, Chemistry Department, Chinese Academy of Science, Beijing and was used without further purification. DNA bases adenine (99%), adenosine (99%), thymine (97%), and thymidine (99%), purchased from Alfa-Aesar, were also used as received.

All experiments were carried out at room temperature in buffered aqueous solutions. The buffer solutions (0.01 mol L^{-1}) employed, covering the pH range from 3.0 to 11.0 with (a) HCl–KH_2PO_4, pH = 3.0–5.0; (b) KH_2PO_4–Na_2HPO_4, pH = 5.0–9.0; (c) Na_2HPO_4–NaOH, pH = 9.0–11.0, pH = 2.0 and pH = 12.0, were adjusted with HCl and NaOH, respectively. The pH value was checked with a WTW-522 pH meter. Double distilled water was used to prepare the samples.

Spectroscopic Methods. Absorption spectra were recorded with a Shimadzu UV-3101-PC spectrometer. Transient absorption spectra were obtained by time-resolved laser spectroscopy using a Lambda Physik LPX-120 XeCl excimer laser (308 nm, pulse energy up to 100 mJ, pulse width 10 ns). The monitoring system included a 150 W xenon lamp; a Hamamatsu R928 photomultiplier tube; a OBB/PTI monochromator, model 101/102; and a digital storage oscilloscope, 9410A LeCroy. The irradiation was carried out in a 1×1 cm^2 rectangular quartz cell. All solutions were treated identically and deoxygenated by bubbling with high-purity argon for 15 min.

Cyclic Voltammetry. Cyclic voltammetric measurements were performed with an Autolab-PGES AUT 73227 potentiostat (Metrohm). A three-electrode cell configuration was used: a Pt counter electrode, a Ag/AgCl reference electrode, and a glassy carbon working electrode (0.03 cm^2 area). The working electrode was polished with diamond paste in water after each single scan to remove possible follow-up products of the oxidative process on the electrode surface. The background current was always subtracted from the current response for further calculation.

■ ASSOCIATED CONTENT

Ⓢ Supporting Information

Additional information as noted in text. This material is available free of charge via the Internet at http://pubs.acs.org.

■ AUTHOR INFORMATION

Corresponding Author
*E-mail: (T.X.N.) nxt-fct@mail.hut.edu.vn, (G.G.) grampp@ tugraz.at.

Present Address
¶School of Chemical Engineering, Hanoi University of Technology, Vietnam

Notes
The authors declare no competing financial interest.

■ ACKNOWLEDGMENTS

■ REFERENCES

(1) Schuster, G. B. *Acc. Chem. Res.* **2000**, *33*, 253−260.

(2) Giese, B. *Acc. Chem. Res.* **2000**, *33*, 631−636.

(3) Genereux, J. C.; Barton, J. K. *Chem. Rev. (Washington, DC, U. S.)* **2010**, *110*, 1642−1662.

(4) Kumar, A.; Sevilla, M. D. *Chem. Rev. (Washington, DC, U. S.)* **2010**, *110*, 7002−7023.

(5) Sengupta, T.; Dutta Choudhury, S.; Basu, S. *J. Am. Chem. Soc.* **2004**, *126*, 10589−10593.

(6) Bose, A.; Sarkar, A. K.; Basu, S. *Biophys. Chem.* **2008**, *136*, 59−65.

(7) Inbar, S.; Linschitz, H.; Cohen, S. G. *J. Am. Chem. Soc.* **1981**, *103*, 7323−7328.

(8) Hurley, J. K.; Linschitz, H.; Treinin, A. *J. Phys. Chem.* **1988**, *92*, 5151−5159.

(9) Marciniak, B.; Bobrowski, K.; Hug, G. L. *J. Phys. Chem.* **1993**, *97*, 11937−11943.

(10) Marciniak, B.; Bobrowski, K.; Hug, G. L.; Rozwadowski, J. *J. Phys. Chem.* **1994**, *98*, 4854−4860.

(11) Bobrowski, K.; Hug, G. L.; Marciniak, B.; Kozubek, H. *J. Phys. Chem.* **1994**, *98*, 537−544.

(12) Encinas, M. V.; Wagner, P. J.; Scaiano, J. C. *J. Phys. Chem.* **1980**, *102*, 1357−1360.

(13) Andrews, L. J.; Levy, J. M.; Linschitz, H. *J. Photochem.* **1976**, *6*, 355−364.

(14) Yurkovskaya, A. V.; Snytnikova, O. A.; Morozova, O. B.; Tsentalovich, Y. P.; Sagdeev, R. Z. *Phys. Chem. Chem. Phys.* **2003**, *5*, 3653−3659.

(15) Christensen, J. J.; Rytting, J. H.; Izatt, R. M. *J. Phys. Chem.* **1967**, *71*, 2700−2705.

(16) Blanco, S. E.; Almandoz, M. C.; Ferretti, F. H. *Spectrochim. Acta, Part A* **2005**, *61*, 93−102.

(17) Sauberlich, J.; Brede, O.; Beckert, D. *Acta Chem. Scand.* **1997**, *51*, 602−609.

(18) Haldar, M.; Chowdhury, M. *Chem. Phys. Lett.* **1999**, *312*, 432−439.

(19) Jackson, G.; Porter, G. *Proc. R. Soc. London, Ser. A* **1961**, *260*, 13−30.

(20) Tsentalovich, Y. P.; Morozova, O. B.; Yurkovskaya, A. V.; Hore, P. J.; Sagdeev, R. Z. *J. Phys. Chem. A* **2000**, *104*, 6912−6916.

(21) Costentin, C.; Robert, M.; Saveant, J.-M.; Teillout, A.-L. *Proc. Natl. Acad. Sci. U.S.A.* **2009**, *106*, 11829−11836.

(22) von Sonntag, C. *Free-Radical-Induced DNA Damage and Its Repair*; Springer: Berlin, 2006; Chapter 10; p 219.

(23) Costentin, C.; Louault, C.; Robert, M.; Saveant, J.-M. *Proc. Natl. Acad. Sci. U.S.A., Early Ed.* **2009**, *106*, 18143−18148.

(24) Christensen, J. J.; Rytting, J. H.; Izatt, R. M. *Biochemistry* **1970**, *9*, 4907−4913.